PROBLEMY MECHATRONIKI
UZBROJENIE, LOTNICTWO, INŻYNIERIA BEZPIECZEŃSTWA

ISSN 2081-5891

9, 1 (31), 2018, 9-22

PROBLEMS OF MECHATRONICS
ARMAMENT, AVIATION, SAFETY ENGINEERING

External Ballistics Simplified Model of the "RT – 400" Rocket Aerial Target

Algimantas FEDARAVIČIUS, Saulius RAČKAUSKAS*, Arvydas SURVILA, Aistis ŠAMELIS

Kaunas University of Technology, Institute of Defence Technologies,
27 Kęstučio Str., LT-44025 Kaunas, Lithuania,
**Corresponding author's e-mail address: saulius.rackauskas@ktu.edu*

Received by the editorial staff on 30 May 2016
Reviewed and verified version received on 21 July 2017

DOI 10.5604/01.3001.0011.7175

Abstract. "RT-400" rocket aerial target system is described in the paper; research method of its simplified external ballistics characteristics is presented and the obtained results are discussed. This system was designed, tested, and produced by a research team of the Institute of Defence Technologies at Kaunas University of Technology and successfully implemented in practice. One of main aims of this paper was to develop external ballistics' model of a rocket propelled aerial target which would enable obtaining various ballistic parameters of the investigated vehicle such as its acceleration, velocity, flight angle, flight range and trajectory using as input the internal ballistics data obtained at earlier experimental research of the "RV-12K" rocket motor in a static horizontal test stand for thrust measurements and determination of other internal ballistics' characteristics such as combustion chamber temperature and pressure.

This work has been compiled from the paper presented during the 11th International Armament Conference on *Scientific Aspects of Armament and Safety Technology*, Ryn, Poland, 19 - 22 September 2016.

During the experimental research process of the vehicle, under test site conditions, the main aim was to compare accuracy of the obtained external ballistics simulation data with the data obtained during experimental approaches using additional measurement techniques such as radar tracking and crash site and launch site GPS coordinates marking.
Keywords: mechanics, rocket motor, air defense, external ballistics, aerial target RT-400

1. INTRODUCTION

Aerial targets are widely used in "Stinger" air defence system training scenarios for various types of military air defence training exercises. For this purpose, three types of aerial targets are mostly used. Stationary (ground or naval), unmanned aerial vehicles (UAV) or rocket propelled targets. Stationary targets are mostly used at the very beginning of the training program, where air defence operators must learn basics about target acquisition, locking and termination. However, if there is the need to acquire a higher qualification, more advanced and more complex aerial target systems have to be used in the training process.

Nowadays, almost all employed aerial targets are unmanned aerial vehicles: they can be drones, airplanes or even various parachute systems. All these mentioned above methods are less effective and uncompetitive in situations where there is a need to simulate a high-speed hostile airplane because of the nature of the airfoil, or because of the unsatisfactory flight range characteristics displayed by drones in their capabilities to perform acute turns and powered banking. It is worth noting that many unmanned aerial vehicles must be controlled by highly skilled operator-pilots, because majority of the drones are unable to withstand bad weather conditions. The most effective way to simulate hostile aircraft (fighter jets, propeller planes, helicopters or drones) is an aerial target which has rocket propulsion system. In the process of such target development, one type of research is mainly based on rocket motors and rocketry systems. Even in UAV operations, rocket boosters are used to launch the aircraft from the ground. The use of rocket motors in aerial target systems can fulfill and simplify various demands based on target dimensions and shapes intended to mimic specific aircraft models or even to fly at similar cruising speeds for some period of time.

Maintaining nominal rocket motor performance through the flight is a challenge often encountered in the field of rocket science [1]. This adds to the problems where internal ballistics is the one of the primarily parts of the equation. There are two basic key elements in a simplified form which allow determining performance characteristics of a rocket motor - thrust, pressure.

The method and research results of external ballistics' characteristics of the "RT-400" rocket aerial target system is discussed in this paper.

Fig. 1. "RT – 400" Aerial target system and pitch plane force diagram

One of the main aims was to develop external ballistics simulation of the aerial target which would enable to obtain various ballistic parameters of the investigated vehicle: acceleration, velocity, flight angle, horizontal and vertical displacement, flight range and safety parabola using as input data the parameters of internal ballistics obtained from the earlier experimental research of the "RV-12K" [2] rocket motor (Fig. 2) which was launched from a static horizontal test stand for thrust measurements and determination of other internal ballistics characteristics such as combustion chamber temperature and pressure [3, 4]. The rocket motor contains 7 main parts. Igniter 1 is used to inject hot gases into combustion chamber where fuel grain 4 is located. O rings 6 and gasket 5 are used for tight sealing of the combustion chamber.

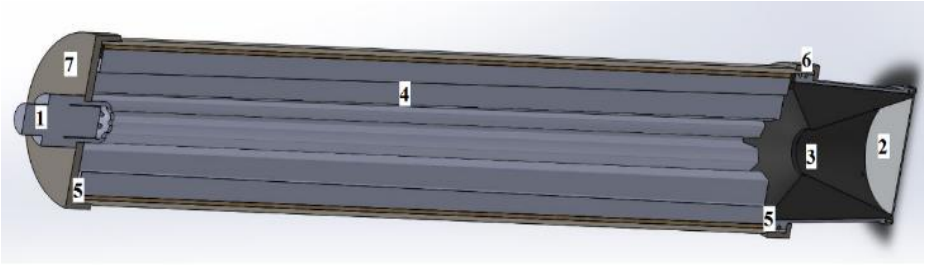

Fig. 2. Rocket motor assembly: 1 – igniter; 2 – end cap; 3 – nozzle; 4 – propellant grain; 5 – hermetic rings; 6 – fixing ring; 7 – top cap

Top cap 7 is used to hold in place igniter 1, gaskets 5, fuel grain 4. Nozzle 3 is used with end cap 2 for better performance of the rocket motor and better pressure buildup after initiation of igniter 1. Using two experimental aerial target prototypes in testing site conditions, the main aim was to compare accuracy of the model with the data obtained during the experiment. Properties of the "RT-400" aerial target system is provided in the table below.

Table 1. Properties of the "RT-400" aerial target system

No.	Property	Values	No.	Property	Values
1.	Length of the target, l [m]	5.2	9.	Rocket motor mass (with propellant), m_{mot} [kg]	35
2.	Length of the rocket motor, l_1 [m]	1.06	10.	Rocket mass, m [kg]	105
3.	Diameter of the target, d [m]	0.4	11.	Burn time of the rocket motor, t_{burn} [s]	3.25
4.	Diameter of the rocket motor, d_1 [m]	0.16	12.	Maximum flight time of the rocket, t_{max} [s]	44.92
5.	Nominal thrust of the rocket motor, T_{nom} [KN]	10	13.	Maximum flight range, X_{max} [km]	4.5
6.	Impulse of the rocket motor, I [KN]	32	14.	Maximum flight height, Y_{max} [km]	2.2
7.	Specific impulse of the rocket motor, I_{sp} [s]	182	15.	Velocity range of the rocket, v [m/s]	30 – 282
8.	Propellant mass, m_{prop} [kg]	18	16.	Drag coefficient, c_d [/]	0.486

Experimental data of velocity and height were obtained with the help of "Giraffe Mk IV" air defence surveillance radar [5]. The crash site was investigated for registration of the touchdown debris. The landing area was monitored by various high-speed video recording devices. From the launch location, for monitoring of the stabilization system (fins), high definition video cameras were used to observe whether the aerial targets were rolling about their axes. The video data was also employed to register the actual time of the aerial target flight from its lift-off to touchdown and to compare it with the calculated data from the model.

Along with all the main aims mentioned above, the most important parameters in modelling of external ballistics were: rocket motor thrust (obtained from the static test stand), motor mass, fuel burn rate, air conditions (obtained from the forecast), geometry of the stabilization system (fins), nose geometry, launch angle, center of gravity (CG), and the center of pressure (CP).

In this design, the neutral star type of propellant grain was used (Fig. 3) [6]. This means that surface area of the burning propellant is constant or deviates very little despite time increment, until sliver of the propellant is reached. To determine the desired rocket motor thrust characteristics, it is crucial to choose right cross section geometry of the propellant grain and to establish the necessary area of burning surface because rocket motor thrust is directly related with propellant grain area A_s Eq. (1) (Fig. 4) [7,8].

$$\int A_s dt = T \tag{1}$$

Fig. 3. Propellant grain during burning

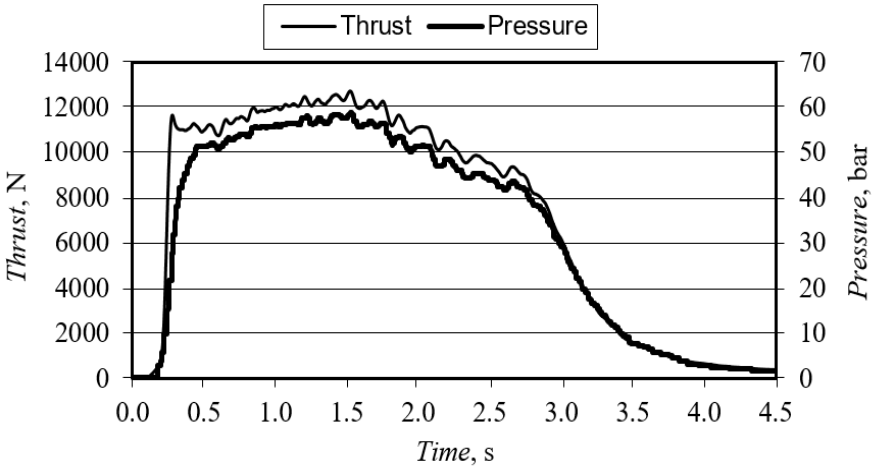

Fig. 4. Motor thrust and pressure versus time experimental dat

2. METHOD AND MODEL

In real world, all processes can be described as 3 dimensional, but to simplify complexity of the model it is assumed that the rocket does not move in Z axis. This assumption can be made because velocity of the rocket in Z axis is insignificant, compared to its velocities in X and Y axes. From the data of experimental research of the rocket motor (Fig. 4), which was used in "RT-400" aerial target, its total (2) and specific (3) impulses were calculated [9].

$$I = F\Delta t = \int F dt = \int \dot{m} \cdot v_{eq} dt = m \cdot v_{eq} \tag{2}$$

where, ṁ – mass flow rate, v_{eq} – equivalent exit velocity.

$$I_{sp} = \frac{I}{m \cdot g_0} = \frac{v_{eq}}{g} = \frac{F}{\dot{m} \cdot g_0} \tag{3}$$

where, g_0 – gravitational constant = 9.81 m/s^2.

Then, three main forces were calculated. Thrust force (4) is presented in Fig. 5, drag force (5) in Fig. 6 and gravity force (6) in Fig. 7.

$$\overrightarrow{F_T} = \dot{m} \cdot \overrightarrow{v_e} + (p_e - p_0) \cdot A_e \tag{4}$$

where, v_e – gas exit velocity, p_e – gas exit pressure, p_0 – atmospheric pressure – 101.3 KPa, A_e – exit area.

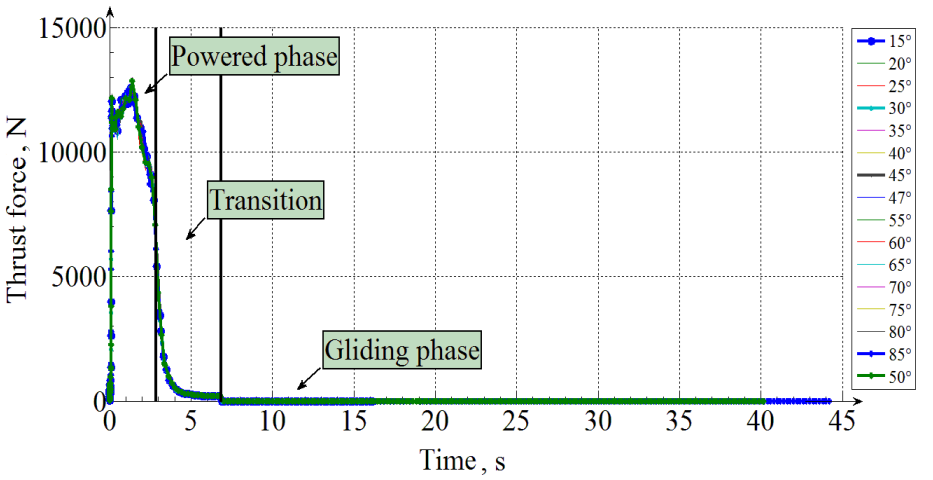

Fig. 5. Aerial target thrust force obtained from simulation.

$$\overrightarrow{F_D} = \frac{1}{2} \cdot \rho \cdot \overrightarrow{v^2} \cdot c_d \cdot A \tag{5}$$

where, ρ – air density – 1.225 kg/m^3, v – velocity, c_d – drag coefficient, A – cross-section area.

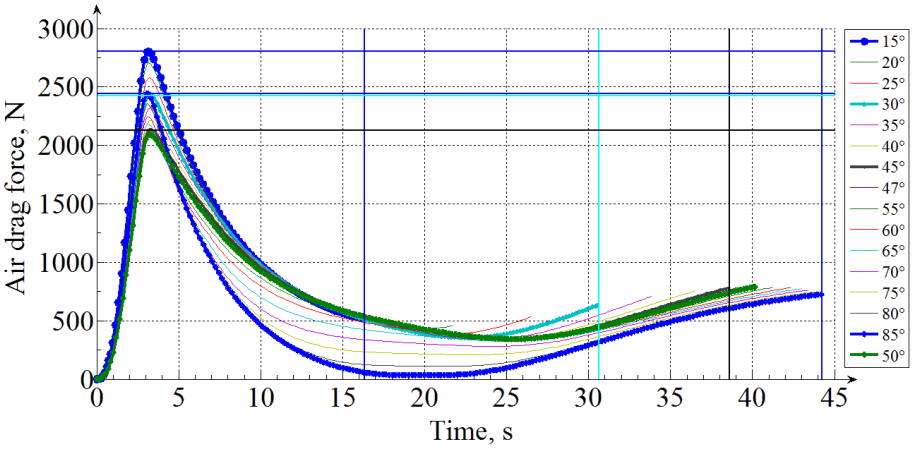

Fig. 6. Aerial target drag force obtained from simulation at different launch angles

$$\overrightarrow{F_G} = m \cdot \vec{g} \tag{6}$$

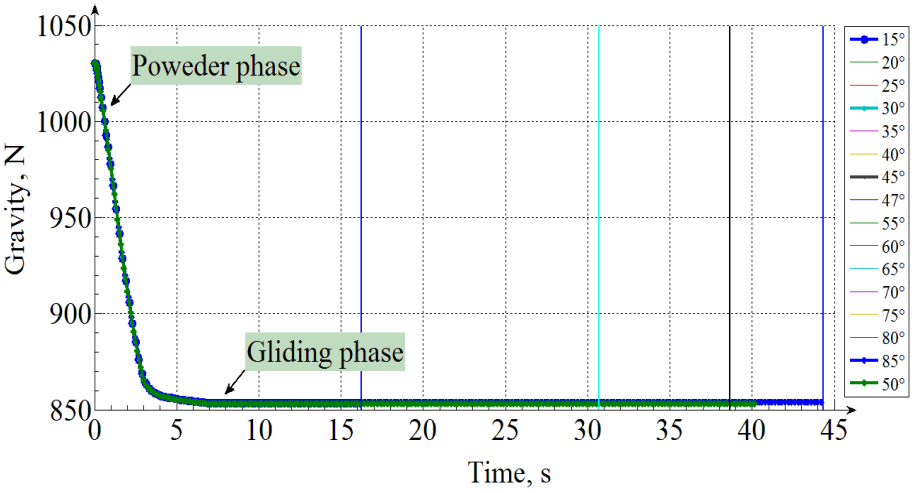

Fig. 7. Aerial target gravity force obtained from simulation

After calculating the force vectors, acceleration can be derived. From the general form of Eq. (7) and the unpowered flight Eq. (8) can be used, depending on the model design. Figure 8 shows the aerial target's acceleration depending on various launch angles. It must be noted that acceleration in Fig. 8 is represented as modulus.

$$\vec{a} = \frac{d\vec{v}}{dt} = \vec{g} = -g \cdot \overrightarrow{1_y} \rightarrow \begin{cases} \frac{dv_x}{dt} = 0 \\ \frac{dv_y}{dt} = -\vec{g} \end{cases} \tag{7}$$

$$|\vec{a}| = \frac{\overrightarrow{F_G} + \overrightarrow{F_D}}{m} = \frac{m \cdot \vec{g} - \left(\frac{\rho \cdot v^2}{2}\right) \cdot \left(\frac{\pi \cdot d^2}{4}\right) \cdot c_{d_0} \cdot \overrightarrow{1_v}}{m} = \vec{g} - \frac{\pi \cdot d^2 \cdot \rho \cdot c_{d_0}}{8 \cdot m} \cdot \vec{v} \cdot v_y \tag{8}$$

where, F – resultant force.

$$\sum F_x = -F_{D_x} + F_T \cdot \cos(\alpha + \varphi) \tag{9}$$

$$\sum F_y = -F_{D_y} - F_G \cdot \sin(\gamma) + F_T \cdot \sin(\alpha + \varphi) \tag{10}$$

where, φ – launch angle, α – angle of the thrust vector referred from the vehicle axis of rotation, γ – angle of the gravity vector depending on the ground plane.

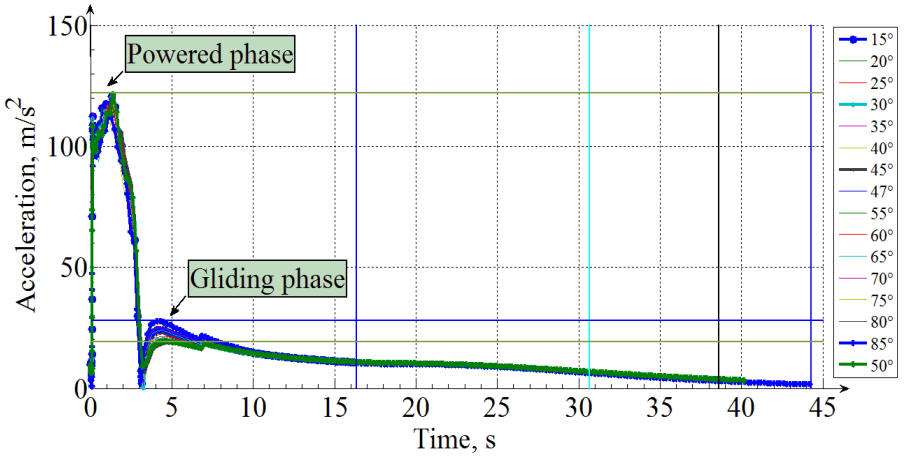

Fig. 8. Aerial target acceleration obtained from simulation at different launch angles

After acceleration of the body, depending on two-dimensional plane axis, its velocity was calculated. Equations (9) and (10) are converted into Eq. (11) which is implemented in the model. Figure 9 shows how velocity of the vehicle is dependent on different launch angles. The end of the curve indicates its touch down to the surface by the target. This index indicates the exact time of touch down. Input data for velocity magnitude (12) and Eq. (13) which were implemented into Matlab® Simulink® were taken from acceleration calculation module.

$$\begin{cases} v_x = \overrightarrow{v_i} \cdot \cos(\varphi), \\ v_y = -\vec{g} \cdot t + \overrightarrow{v_i} \cdot \sin(\varphi), \end{cases} \tag{11}$$

where $\overrightarrow{v_i}$ – initial velocity or velocity after each time period, φ – launch angle in degrees.

$$|v| = \sqrt{v_x^2 + v_y^2} \tag{12}$$

$$\vec{v} = \int_0^t \vec{a}\, dt \tag{13}$$

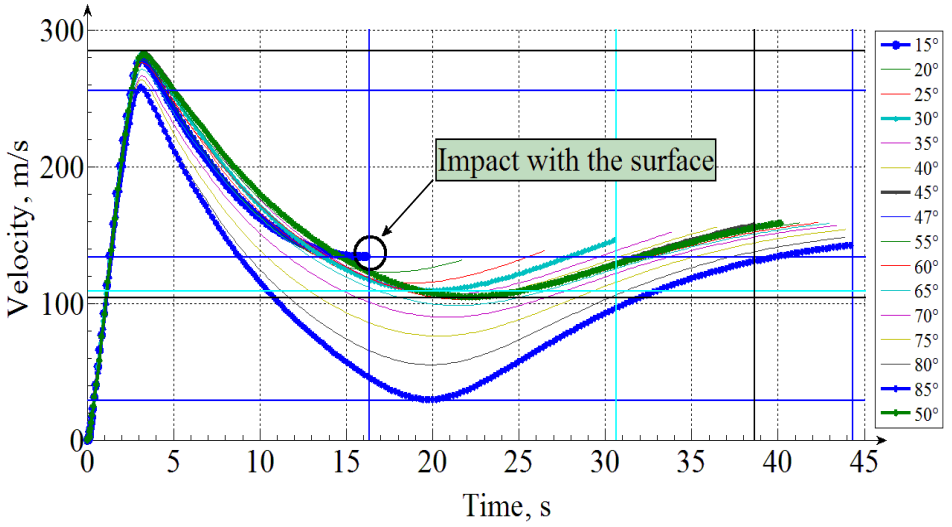

Fig. 9. Aerial target velocity obtained from simulation at different launch angles.

The angle of the flight path for the parabolic trajectory is determined by Eq. (14) and is shown in Fig. 10. This parameter is needed to determine at which time instant the target will reach its apogee. As it is seen in Fig. 9, it also shows the time of touch down.

$$\theta = \left| \left| \tan^{-1}\left(\frac{v_x}{v_y}\right) \right| \cdot \frac{180}{\pi} \right| \tag{14}$$

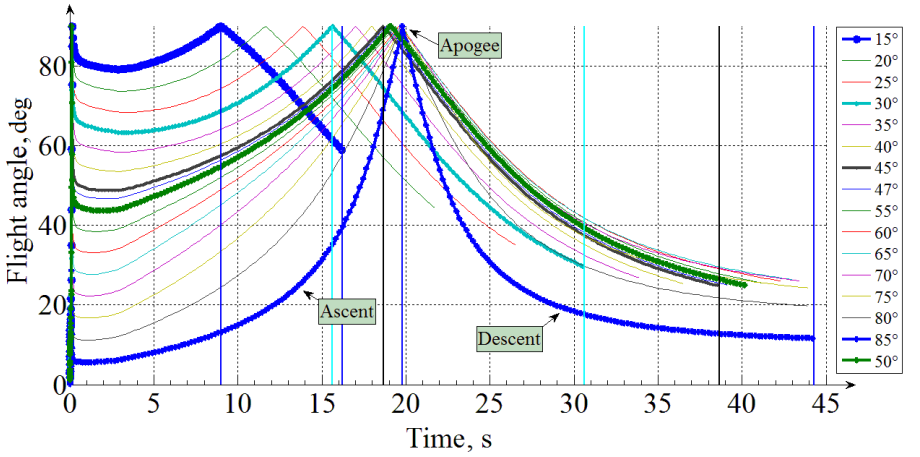

Fig. 10. Aerial target flight angle obtained from simulation at different launch angles

By integrating the velocity, the path is determined from Eq. (15). For different axes, the path of the aerial target is obtained using Eq. (16). Figure 11 illustrates trajectory of the aerial target at different launch angles. Two characteristic points are marked on the 30°-trajectory. These points mark the places where the targets were shot down during firing exercises – experiments by the operator of the "Stinger" anti-air missile defence system of the Air Defence Battalion of the Lithuanian Air Forces [10].

$$s = \int_0^t \vec{v}\ dt = \int_0^t \overrightarrow{v_i} + at\ dt \tag{15}$$

$$\begin{cases} x = v_x \cdot t \cdot \cos(\varphi) \\ y = -\dfrac{g \cdot t^2}{2} + v_y \cdot t \cdot \sin(\varphi) \end{cases} \tag{16}$$

The experiment was performed to evaluate the reliability and precision of the model. For that purpose, two aerial target prototypes were used. In Table 1, comparison of the simulation results and testing data is presented. At the 30° launch angle, the aerial target impacted the surface after 4050 m, while the calculated distance was 4000 m. During the second attempt, when the launch angle of the prototype was 45°, flight range of the vehicle was 4250 m, while the calculated distance was 4450. In the first case, the error of simulation results in comparison with experimental results of the aerial target flight range was 50 m or 1.25% and in the second case, the error was 200 m or 4.7%. Based on these results, the calculated accuracy of the model does not exceed 5% threshold.

Table 1. Experimental and calculated data

	Range (model), m	Range (experimental), m	Error, %
Target #1	4000	4050	1.25
Target #2	4450	4250	4.7

During the "Amber arrow 2014" firing exercises at sea, the aerial target was sought by the operator of the "Stinger" missile air defence system and got hit with the first shot in 18.5 seconds after launch of the aerial target at the launch angle of 30°. The target was terminated at 2950 m from the launch site. After the second launch of the aerial target, it was terminated after 25 seconds. The target was hit at 3580 m from the launch site.

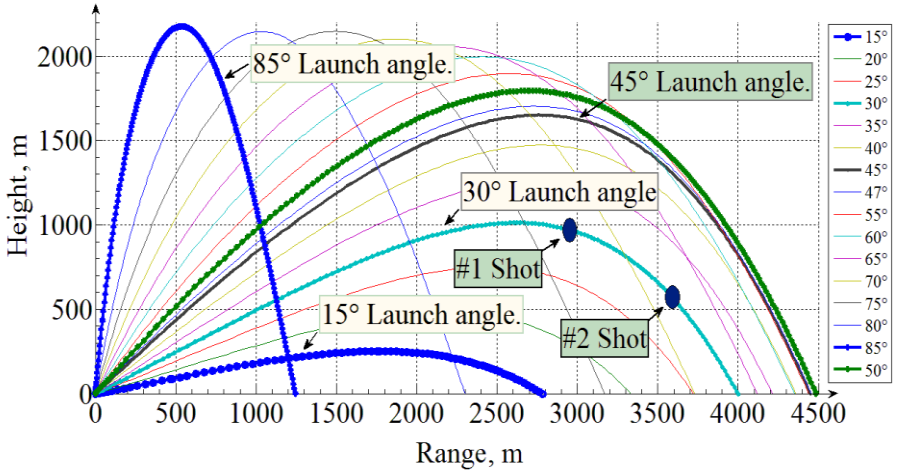

Fig. 11. Aerial target trajectory calculated using the model at different launch angles

Results of the model were compared with the experimental results that were obtained using air defence surveillance radar (Fig. 12). In comparison of the data from the radar with the model data, when the aerial target was launched at 30°angle, it can be concluded that the model results are accurate and show good correlation with the experimental data.

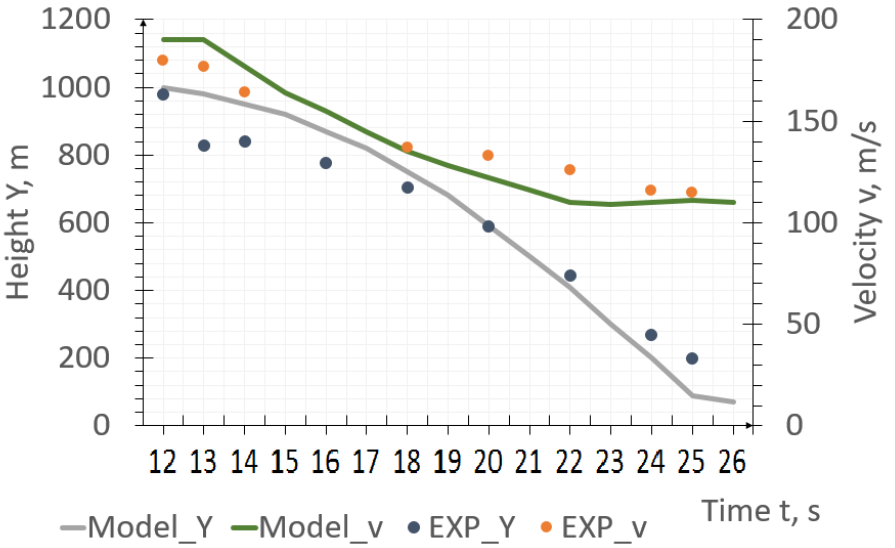

Fig. 12. Radar and model comparison graphs

3. CONCLUSIONS AND FINAL REMARKS

The model for determining external ballistics' characteristics of the "RT-400" rocket propelled aerial target was developed. It includes determining the parameters such as thrust, gravity, and air drag forces which influence behavior of the aerial target. The thrust force in all cases, performed at different launch angles, was the same, because the model was designed using the same rocket motor and its parameters. The gravity force was also the same in all cases. The range of the drag force, right after the powered flight mode was from 2010 N when the launch angle was 50° to 2800N when launch angle was 15°. In its powered flight mode, the aerial target acceleration was approximately 120 m/s^2 at every launch angle case. In its gliding phase, the acceleration of the aerial target, considering the launch angle, was between 20-30 m/s^2. The highest and lowest possible aerial target speeds were observed at the smallest admissible launch angle of 15°. After the powered phase, had just ended, the speed of the aerial target was 280 m/s and 135 m/s before impact with the surface.

Given the steepest launch angle at 85°, the aerial target speed just after the powered phase was 260 m/s, 30 m/s at the apogee, and was 140 m/s just before impact with the surface. Given the standard launch angles of 30° and 45°, the speeds of the aerial target, after the powered phase ended up, were almost the same in both cases, 280 m/s, however, after apogee was reached, the speed was 105 m/s and 110 m/s, respectively and before impact with the surface – 148 m/s and 160 m/s. At a launch angle of 15°, the aerial target reached its apogee in the 9th second of its flight, while at an 85° angle it reached its apogee in the 20th second of its flight. Given the standard launch angle of 30°, the aerial target reached its apogee after 15.5 seconds of flight, and given an angle of the 45° - 19 seconds. The flight times of the aerial target at the steepest and lowest angles were 16 and 44 seconds, respectively and given the standard angles – 30.5 and 48.5 seconds. The model results indicate that at a 15° launch angle, the apogee of the aerial target was at 250 m with a flight range of approximately 2800 m. At an 85° launch angle, the apogee was reached at 2200 m and the range of the flight was approximately 1250 m. Given the standard launch angles, the apogee was reached at approximately 1000 m with a range of 4000m respectively. Given 45° angle, the apogee was reached at 1650 m and the range was 4450 m.

So, the model is adequate for future performance revisions in development of the aerial target systems.

Concluding, it is worth stating that this model, developed by a research team, was intentionally made universal for other research groups to make their own implementations of similar problems more easily. The model provides better understanding of problematic scenarios which can be encountered during similar experimental testing that can consume great part of research, labor time and budget.

ACKNOWLEDGEMENTS

This work was supported by the Research Council of Lithuania, grant No. S-MIP-17-94 "Experimental Rocket: Research and Development".

REFERENCES

[1] Mason D. R., S. L. Folkman, M. A. Behring. 1979. Thrust Oscillations of the Space Shuttle Solid Rocket Booster Motor during Static Tests. In *Proceedings of the 15th Joint Propulsion Conference 79* 1138 : 18-20.

[2] Fedaravičius Algimantas, Saulius Račkauskas, Arvydas Survila, Laima Patašienė. 2015. "Design of the testing system for solid propellant rocket motor thrust measurements using mathematical modelling techniques". *Journal of Measurements in Engineering* 3 (4) : 123‑131.

[3] Ren Zongjin, Baoyuan Sun, Jun Zhang, Min Qian. 2008. The Dynamic Model and Acceleration Compensation for the Thrust Measurement System of Attitude/Orbit Rocket. In *Proceedings of the International Workshop on Modelling, Simulation and Optimization* 30-33.

[4] Gillette O. Larry. 1975. "Measurement of Static Strain at 2,000° F" *Experimental Mechanics* 15 (8) : 316-322.

[5] http://everything.explained.today/GIRAFFE_Radar/ GIRAFFE Radar Explained (Accessed May 24, 2016).

[6] Rafique F. Amer, Qasim Zeeshan, Ali Kamran, Liang Guozhu. 2015. "A New Paradigm for Star Grain Design and Optimization". *Aircraft Engineering and Aerospace Technology* 87 (5) : 476-82.

[7] Hartfield Roy, Rhonald Jenkins, John Burkhalter, Winfred Foster. 2003. A Review of Analytical Methods for Solid Rocket Motor Grain Analysis. Presented at the *39th AIAA/ASME/SAE/ASEE Joint Propulsion Conference and Exhibit*, 2003. DOI:10.2514/6.2003-4506.

[8] De Lucena S.E., M.G. De Aquino, A. Caporalli-Filho. 2005. A Load Cell for Grain-Propelled Ballistic Rocket Thrust Measurement. In *Proceedings of the 2005 IEEE Instrumentation and Measurement Technology Conference* 3 : 1767-772.

[9] Hofer Richard Robert. 2004. *Development and Characterization of High-efficiency, High-specific Impulse Xenon Hall Thrusters*. Washington, DC 20546–0001: National Aeronautics and Space Administration.

[10] http://kariuomene.kam.lt/en/weaponry_and_technology.html. *Weaponry and Technology. Lithuanian Armed Forces* (Accessed May 24, 2016).